Micro-Replication: Precision Metal Parts from Electroformed Master Molds

James J. Kelly, John T. Hachman, and Nancy Y. C. Yang

Sandia National Laboratories

Issued by Sandia National Laboratories, operated for the United States Department of Energy by Sandia Corporation.

Available to DOE and DOE contractors from
    U.S. Department of Energy
    Office of Scientific and Technical Information
    P.O. Box 62
    Oak Ridge, TN 37831

    Telephone: (865)576-8401
    Facsimile: (865)576-5728
    E-Mail: reports@adonis.osti.gov
    Online ordering: http://www.doe.gov/bridge

Available to the public from
    U.S. Department of Commerce
    National Technical Information Service
    5285 Port Royal Rd
    Springfield, VA 22161

    Telephone: (800)553-6847
    Facsimile: (703)605-6900
    E-Mail: orders@ntis.fedworld.gov
    Online order: http://www.ntis.gov/ordering.htm

Micro-Replication: Precision Metal Parts from Electroformed Master Molds

James J. Kelly, John T. Hachman, and Nancy Y. C. Yang
Microsystems Processing Department
Sandia National Laboratories
Livermore, California 94550

Abstract

The possibility of using through-mask electrodeposition to fill features with active sidewalls was investigated. Both metal (Ni) and conductive substrates were employed; the demolding of electroformed Ni metal parts from metal substrates was difficult despite the use of various lubricants. Because of damage to the electrodeposited parts during the demolding process, conductive plastic substrates appear more feasible than metal substrates. Direct current was capable of filling features with low aspect ratios (~2) with only minor voiding. For higher aspect ratio features (~7), pulsed deposition and direct current with the leveling agent coumarin appeared to be more effective than pulsed reverse deposition. Since the characteristic diffusion time constant varies with the square of the feature depth, chloride ions are necessary to prevent passivation during the long pulse off-times required for uniform feature filling through a thick mask. It is shown that although thick masks require long pulse off-times, the recommended deposition rate for uniform filling (available in the literature) should not depend on the mask thickness (although the total deposition time will).

ACKNOWLEDGEMENT

TABLE OF CONTENTS

Micro-Replication: Precision Metal Parts from Electroformed Master Molds

Introduction

Although methods exist to produce plastic microstructures cost-effectively (*e.g.*, hot embossing and injection molding),[1-3] a simple, economical way to produce metallic microstructures has not yet been clearly demonstrated. Thies *et al.* used cluster beams from a nozzle source to deposit Ag at the bottom of features in an injection-molded PMMA substrate.[4-5] This process was followed by conventional Ni electrodeposition into the features after making electrical contact to the Ag clusters (no details as to how this was done are given).[4] Attempts at micro precision casting (using molten metal to fill ceramic molds) and micro metal injection molding (using fine metal powders with binder to fill molds) are summarized by Ruprecht *et al.*[6] These latter two methods, while potentially viable at some point in the future, are in need of further development before they are used on a routine basis for fabrication of metallic microstructures.[7]

Another interesting approach to the problem has been the use of conductive plastic material that may be formed and simultaneously patterned by injection molding. A metal master mold with the desired pattern (formed of Ni or a Ni alloy *via* the conventional LIGA process, for example)[8] is used for the injection molding to transfer the pattern to the conducting plastic material. The

conducting plastic, bearing the desired features, is then used as a substrate for electrodeposition.[6] The plastic mold with the metal microstructures is then planarized, after which the plastic is dissolved in an organic solvent such as acetone. The process is summarized in Figure 1. The advantages of this approach are that no special equipment is necessary and that, as in the conventional LIGA process, electrodeposition is used to form the features. This technique is also known as the "lost mold" process.

PMMA

substrate & metal seed layer

metal substrate with pattern

bonding

injection

conductive plastic

exposure, development

mold release

electrodeposition

planarization

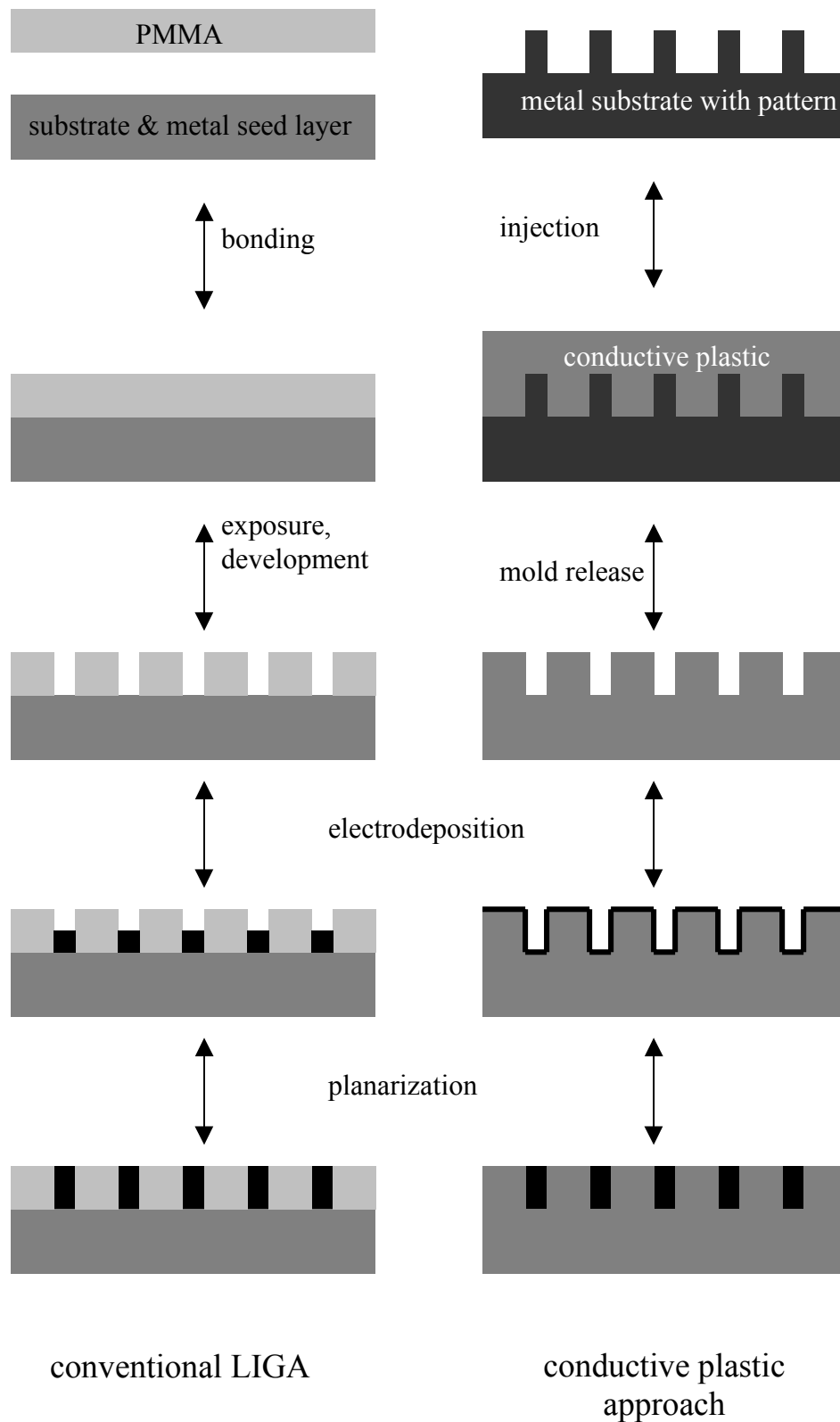conventional LIGA

conductive plastic approach

Figure 1. Comparison of conventional LIGA process flow and electrodeposition on a conductive plastic material with active sidewalls.

6

The problem observed by previous workers with this approach is the presence of voids in the center of the electrodeposited metal microstructures. An important difference between this process and the conventional LIGA process is the presence of active sidewalls when using a conducting plastic; this is also depicted in Figure 1. Hence, the film grows from the sidewalls as well as from the bottom of the feature. Voids result when the upper portion of the feature grows more rapidly than the bottom; the top of the feature may be pinched off when the growing metal fronts from the two sidewalls meet. The replenishment of metal ions from the bulk of the electrolyte to the lower portion of the feature is no longer possible, and a void results.

These previous studies using conductive plastic substrates did not mention the possibility of using pulse plating or additives known as leveling agents to overcome the observed voiding problem. However, pulse plating and leveling agents have been used in copper plating for printed circuit boards to fill features of about 100 microns with active sidewalls.[9] Additives are essential in the electrodeposition of void-free Cu on chip interconnects (in this case the sidewalls are active also, but the length scale of interest is submicron).[10] The classic leveling agent studies in the 1950's and 1960's all dealt with Ni electrodeposition and features on the order of ~100 microns. The most studied leveling agent for Ni is coumarin,[11-12] which does not contain sulfur that can embrittle the deposited metal. In this study we give consideration to these

possibilities to enable void-free feature filling on substrates with active sidewalls.

The possibility of electroplating directly on a metal substrate (fabricated by the conventional LIGA process) is also explored. Separation of the metal microstructures of interest is made possible by chemically treating the metal substrate before electrodeposition.[13] The metal piece with the microstructures would then be potted in a plastic support for subsequent planarization. This process alternative is shown in Figure 2.
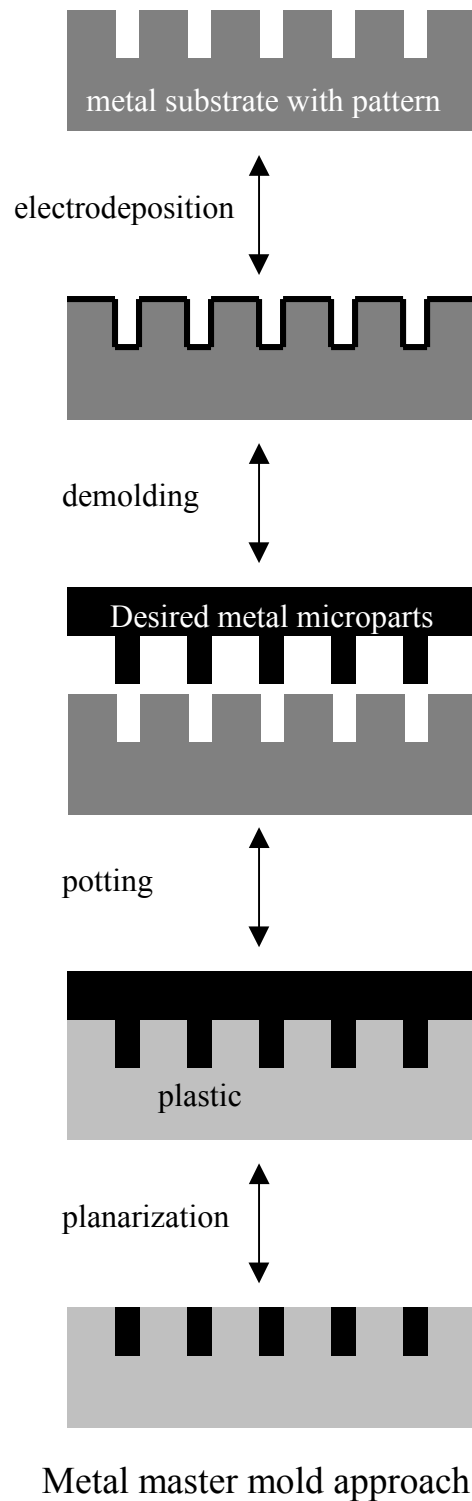
Figure 2. Electrodeposition on a metal master mold with active sidewalls. A chemical treatment of the master mold surface allows for demolding after deposition.

9

Experimental

Features for direct deposition on a metal substrate were produced by through-mask electrodeposition of Ni on a wafer patterned by the LIGA process. The metal was allowed to overplate and join together, forming a solid piece of Ni having various shapes. The smallest features were ~100 μm in width, while the depth of all the features was 150 μm. The metal master mold was then treated in a dichromate solution for 2 minutes to form Ni oxide, enabling subsequent demolding. The lubricants MoS_2 (Rosemill Co., Moli-spray) and WS_2 (Cerac Specialty Inorganics, Inc.) were considered as supplementary treatments to facilitate demolding. Only direct current was employed for experiments on the metal substrate since the features had low aspect ratios and thus are not expected to be difficult to fill. An SEM micrograph of the Ni plated and demolded from the Ni master mold is shown in Figure 3.

Features for electrodeposition on conductive PMMA (doped with Ag particles) were formed by drilling holes into the surface, resulting in trenches ~150 μm wide and 1 mm deep. The dimensions of these features, having an aspect ratio of ~7, were designed to be challenging in order to test the feature-filling capabilities of the four different electrodeposition schemes listed in Table 1, along with corresponding electrolytes. For pulse reverse plating, Cl^- ions were added to the conventional sulfamate electrolyte since they are necessary

for dissolution during the stripping part of the pulse. As the leveling agent coumarin is typically employed with a Watts-type bath, an electrolyte this type was used here for experiments with coumarin. All chemicals were certified ACS grade, and S-depolarized Ni was used as the counterelectrode in a two-electrode arrangement. The pH of all electrolytes was between 3.5 and 4.0. The bulk of the electrolyte was well mixed, but no special measures were taken to attempt to enhance flow into the features. The choice of the pulse parameters is discussed in the following section.
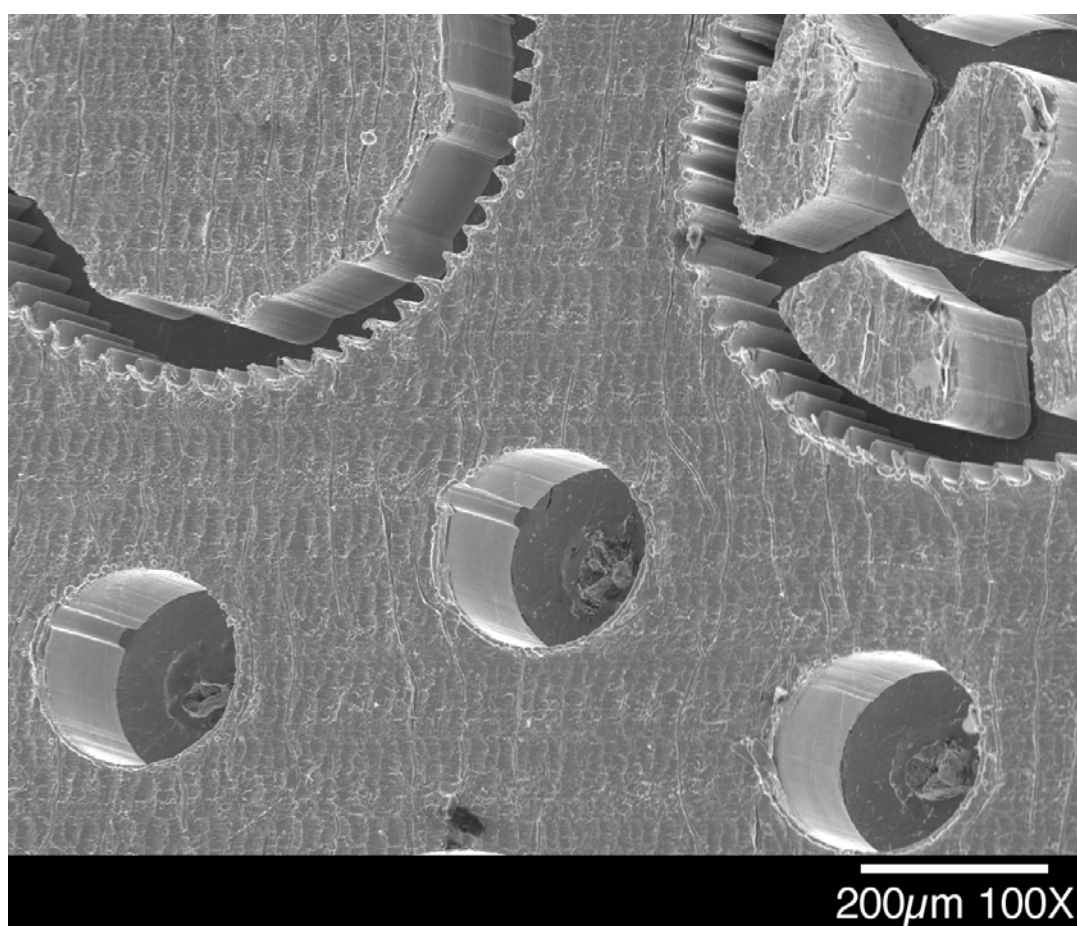

FIGURE 3. SEM micrograph of electrodeposited features after separation from the metal master mold.

Constituent	Direct Current	Pulsed Deposition	Pulse-Reverse Deposition	Leveling Agent
Ni(SO$_3$NH$_2$)$_2$•4 H$_2$O	1.54 M	1.54 M	1.54 M	0
H$_3$BO$_3$ (boric acid)	0.73 M	0.73 M	0.73 M	0.61
NiCl$_2$•6 H$_2$O	0	0	0.03	0.19
NiSO$_4$•6 H$_2$O	0	0	0	1.25
sodium dodecyl sulfate (SDS)	0.2 g/L	0.2 g/L	0.2 g/L	0.2 g/L
coumarin	0	0	0	0.03 g/L
Operating temperature	50 °C	50 °C	50 °C	50 °C
pH (@ 50 °C)	3.5-4.0	3.5-4.0	3.5-4.0	3.5-4.0
i (mA/cm^2)	15	15 (i_{on}) 0 (i_{off})	15 (i_{on}) 0 (i_{off}) -30 (i_{dis})	15

Table 1.   Operating conditions for electrodeposition schemes on conductive PMMA.   Chloride ions are necessary for dissolution of Ni and are hence included for pulse reverse deposition, while the Watts bath chemistry is typically used for Ni deposition with coumarin.

Theory

The diffusion of the Ni^{2+} ions to the bottom of the feature is expected to limit the void-free filling of high aspect ratio features.   Ni^{2+} ions become depleted at the bottom of the feature due to the diffusion distance from the bulk electrolyte; as a result, the local deposition rate is smaller at the trench bottom as compared to near the mouth.   A simple dimensional analysis suggests that, assuming stagnant diffusion within the feature,
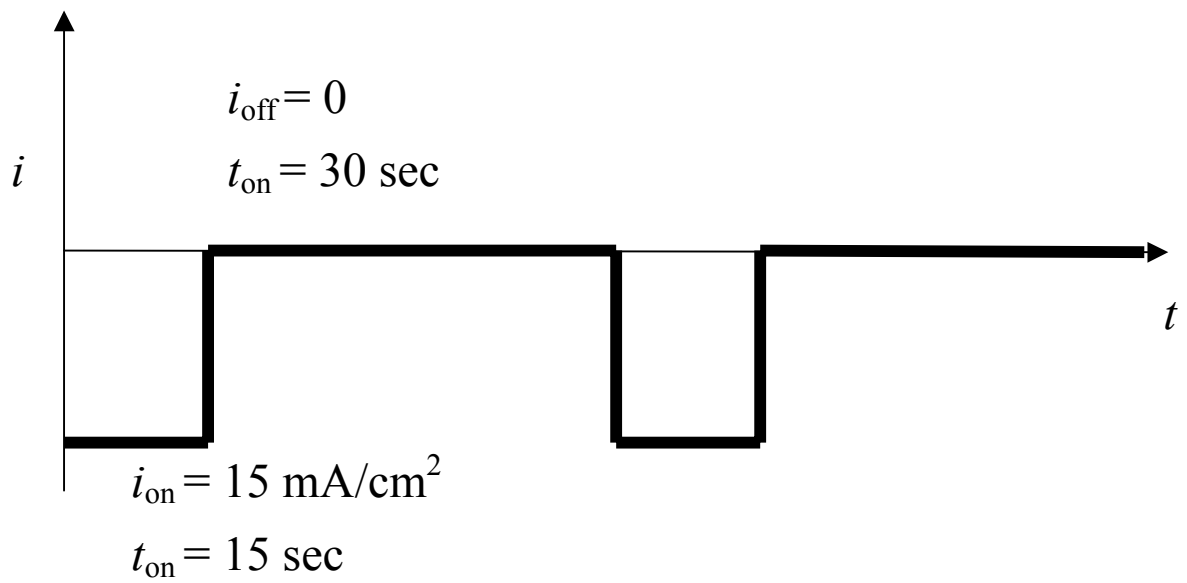
$$\tau \cong \frac{L^2}{D} \qquad\qquad (1)$$

where τ is the characteristic diffusion time constant, L is the feature depth, and D is the diffusion coefficient of the Ni species. For $L = 1$ mm and D ~ 10^{-5} cm²/s for a metal ion in water at 25 °C,[14] $\tau = 1000$ sec. A recent study by West et al.[15] showed that the off-time (t_{off}) should be on the order of the time constant and the deposition time should be smaller than the diffusion time constant for void-free filling of features with active sidewalls.

An interesting observation of equation (1) is that τ (and the pulse off-time if pulsed deposition is used for void-free feature filling) scales with the feature depth to the second power. A two-fold increase in PMMA thickness then results in a four-fold increase in the off-time necessary to uniformly fill the feature; this suggests that this method is better suited to thinner PMMA molds and to electrolytes where pulsing with long off-times is possible. For the conventional sulfamate electrolyte, $t_{off} >$ ~1 minute lead to laminations and possibly poor deposit quality due to passivation during t_{off}. In order to test a conventional nickel sulfamate electrolyte and avoid these complications, a t_{off} value of 30 sec was chosen. We thus expect that the features will not be perfectly filled, but the experimental results will provide valuable information as to how poor the filling performance is; in the case of very non-uniform filling, the electrolyte chemistry will have to be altered to accommodate long t_{off} values (e.g., by adding Cl⁻ ions to prevent passivation).

In Reference 15 it was shown that using pulse reverse plating improves feature-filling performance. This approach was tested here as well; the stripping portion of the wave was enabled by introducing Cl^- ions to the electrolyte, as outlined in Table 1. Figure 4 shows the differences between pulse and pulse reverse plating, along with the details of the pulsing. Apparently the dissolved Ni^{2+} ions within the feature may diffuse down towards the trench bottom, lessening the difference in Ni^{2+} concentration along the trench depth under certain conditions. A more detailed explanation is available in Reference 15.

The efficacy of leveling agents, such as coumarin in this study, depends on mass transport effects. A simple explanation for their observed effects is that they inhibit metal deposition by blocking the surface; since they are consumed at a rate controlled by mass transport, high points on the substrate receive a higher flux of the leveling agent than lower points.[9,11-12] Current for metal deposition is thus diverted towards the low points of uneven surfaces. Modifications to the fluid flow across the wafer may be made to optimize the performance of leveling agents since they are sensitive to transport conditions, but a detailed investigation of this aspect was not attempted here.

Pulsed deposition

$i_{off} = 0$
$t_{on} = 30$ sec

$i_{on} = 15$ mA/cm^2
$t_{on} = 15$ sec

Pulse-reverse deposition

$i_{dis} = 30$ mA/cm^2
$t_{dis} = 1.5$ sec

$i_{off} = 0$
$t_{on} = 30$ sec

$i_{on} = 15$ mA/cm^2
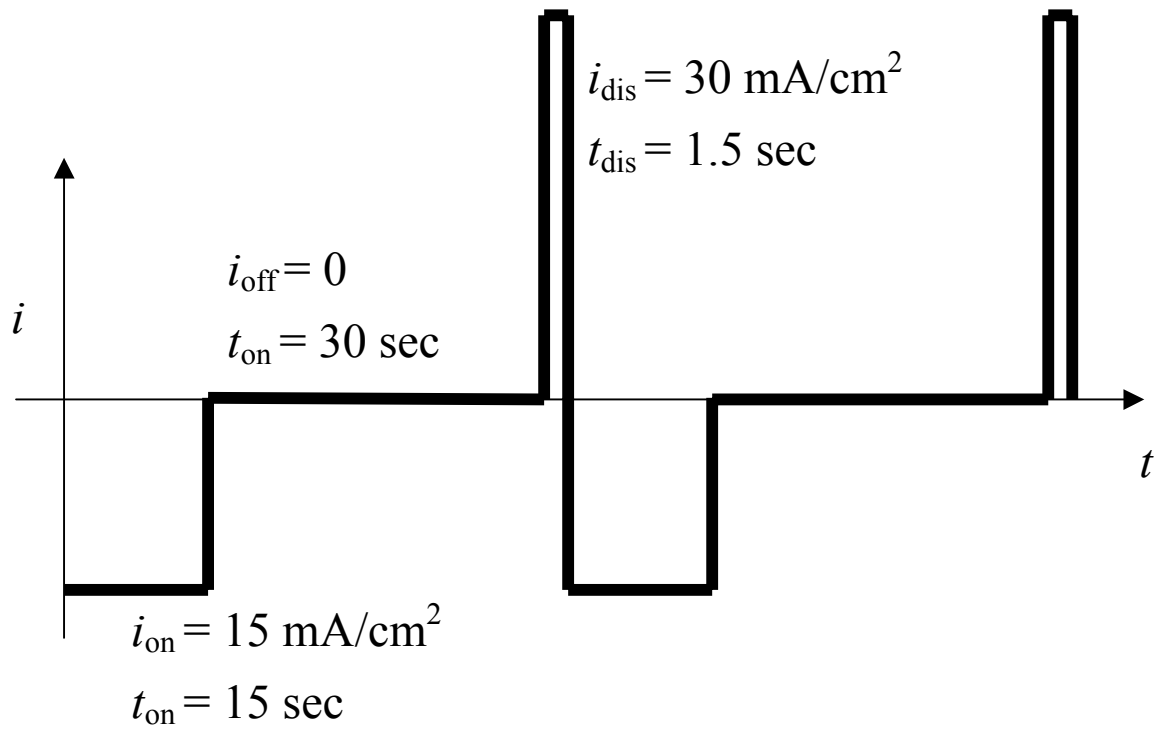$t_{on} = 15$ sec

Figure 4. Schematic illustration of pulse waveforms used in this study.

Results and Discussion

<u>Metal on Metal Deposition</u>

Figures 5a and b show the results of demolding a Ni piece that was plated on a Ni master formed from the conventional LIGA process. Some damage is evident from the mechanical demolding; a fair amount of effort was necessary to pry to two pieces of Ni apart. The supplementary lubricants tried here did not have an appreciable effect on the ease of this operation. White arrows indicate a few missing structures (although several are evident) that were lost presumably during the demolding process. Figure 6 shows a higher magnification view of the demolded piece. It is somewhat surprising that the tooth-like features are still present and are in reasonably good condition, given the harshness of the demolding process. Damage is greatest close to the interface with the Ni master. It is likely that some deformation of the Ni piece shown occurred while some of the teeth were still attached to the master substrate, leading to the cracking apparent in Figure 6.

The separation damage is also evident in cross section. Figure 7 is a cross sectional optical micrograph of a region of the master mold where the two halves did not separate during demolding. Even though direct current was used for the Ni on Ni deposition, the voids are relatively small. This is presumably due to the low aspect ratio and small height of the features. It is interesting to note the difference in grain structure between the master mold and the "daughter" Ni; since the master (the substrate, on the bottom of the micrograph

in Figure 7b) was formed by the conventional LIGA process, the grains in the master rectangular features (those with no voiding) all point vertically, since growth starts only at the bottom of a feature in PMMA. The grains in the rectangular features in the daughter (those showing some voiding), on the other hand, all point to the center of the rectangular features, since growth starts from the sidewalls as well.
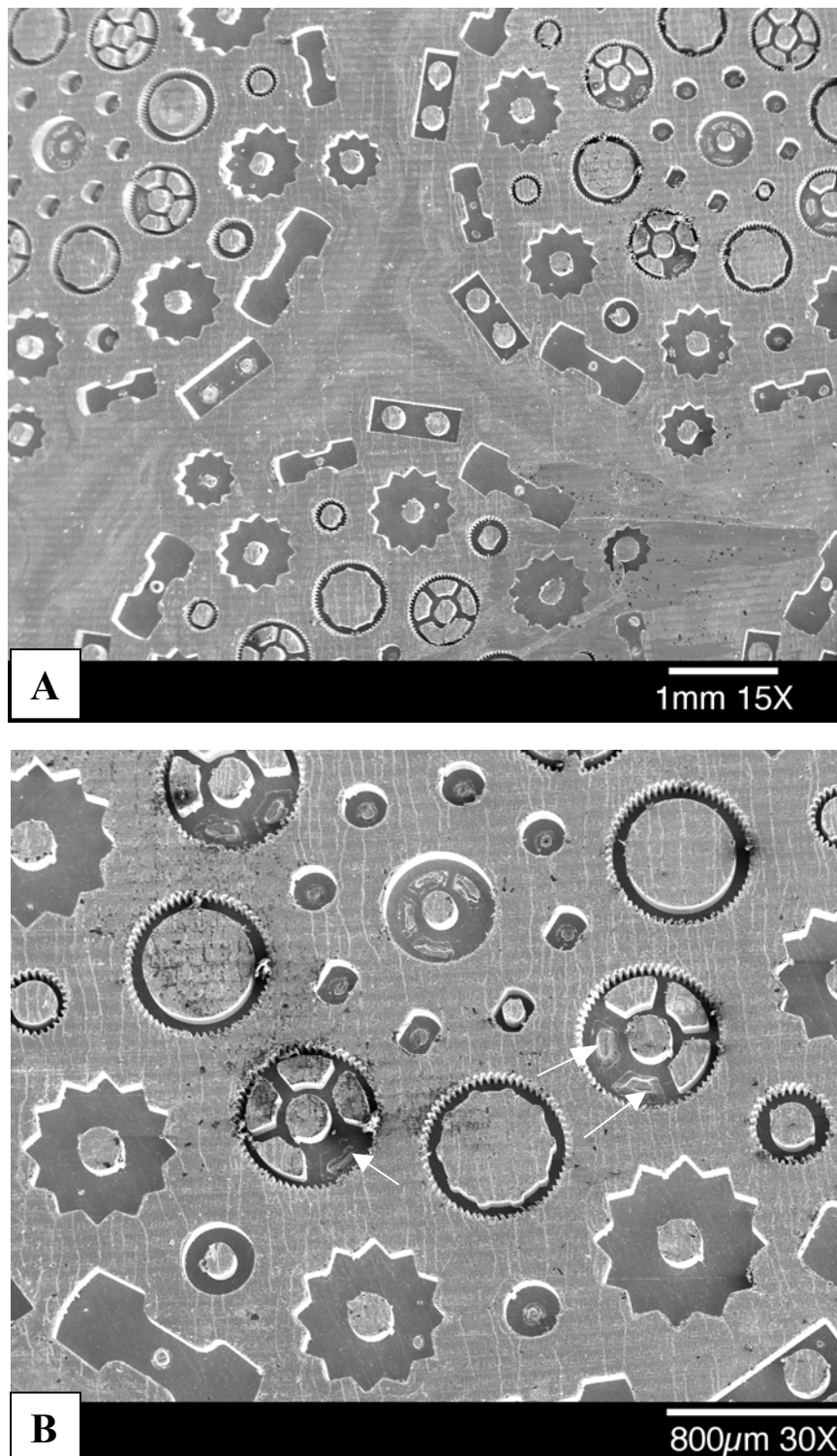
Figure 5a & b. SEM micrographs of Ni piece demolded from Ni master. Damage from the demolding process is evident in B.
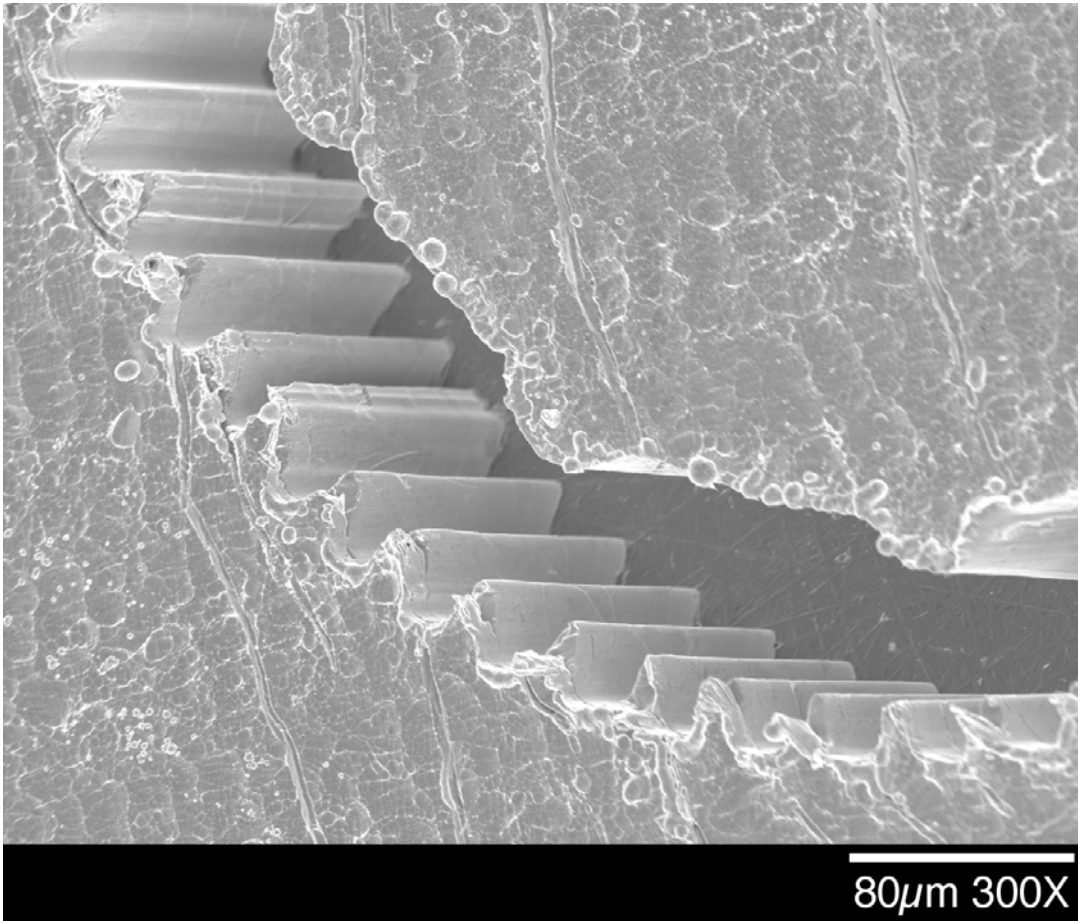
Figure 6. Close up view of teeth-like features on demonlded Ni. At the top of each tooth (close to the interface with the master), it appears that the Ni is cracked and spalled off in some cases.
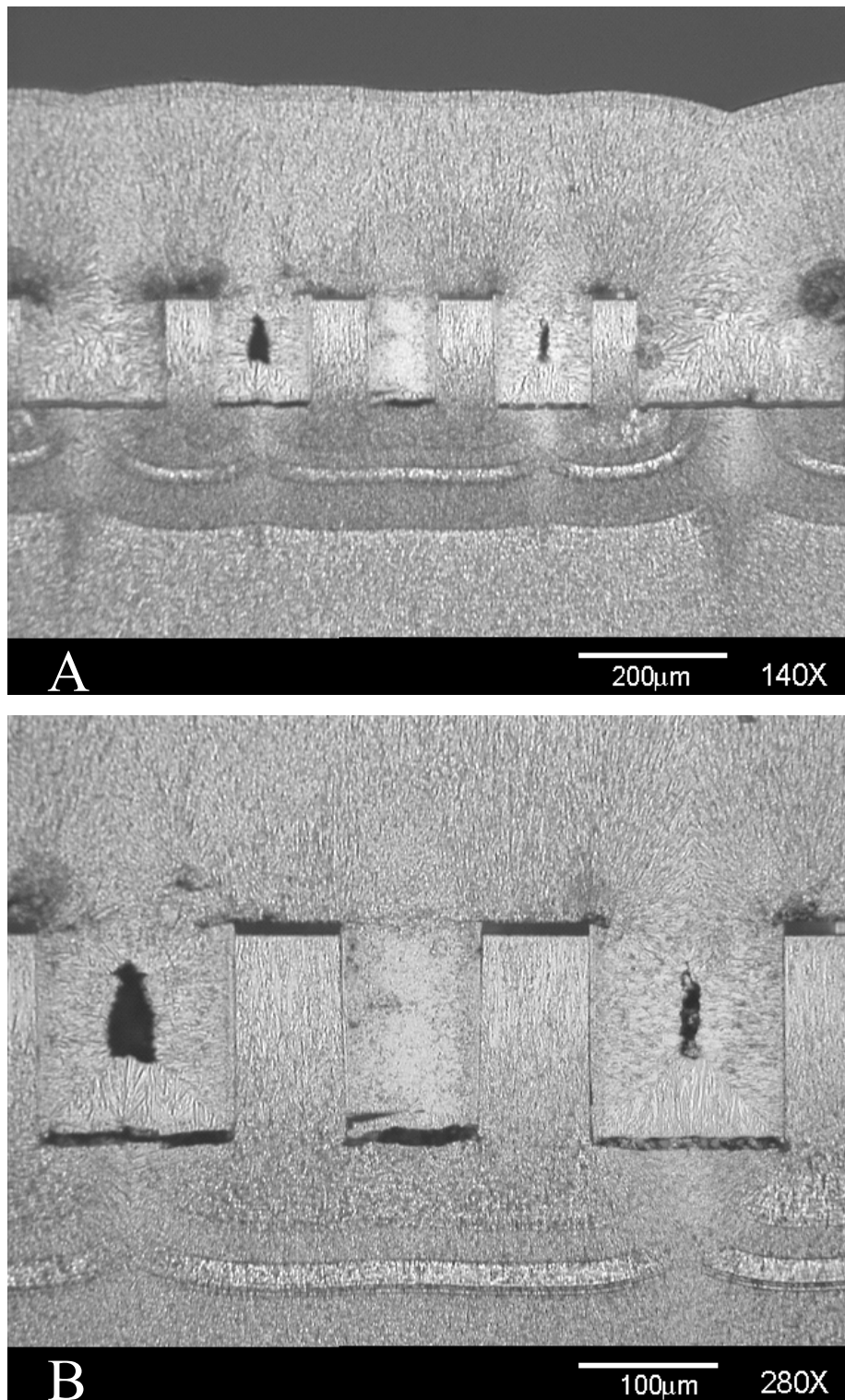
Figure 7a & b. Optical micrograph of electrodeposited Ni on Ni master mold where demolding did not separate the two pieces. Damage from the demolding is evident in the central feature in (b). Voiding is apparent as pulsed deposition was not used. The grain structure clearly shows the film growth and evolution.

Voiding is visible upon polishing the daughter Ni piece from the top and observing the polished features in plan view. Figure 8 is a plan view optical micrograph of the polished Ni daughter piece. Most of the columnar features have some minor voiding. This is not surprising since direct current was used to make the Ni daughter. Equation (1) suggests for this geometry a diffusion time constant of ~23 sec. Reference 5 recommends using $t_{on} < \tau/2$. This leads to a duty cycle (t_{on}/t_{pulse}, where t_{pulse} is the total pulse period) of about 1/3. Since growth occurred from both sidewalls and the deposition rate was about 18 µm/hour, it took approximately 3 hours to fill the 100-µm wide features using direct current. For this geometry, equation (1) predicts that using pulsed deposition to achieve void-free filling would increase the total deposition time to 9 hours, still a reasonable plating time. Since it is the width of the features that determines their filling times, pulsed deposition schemes are better suited to narrow features that still may be filled within a reasonable time despite potentially long off-times and low duty cycles.
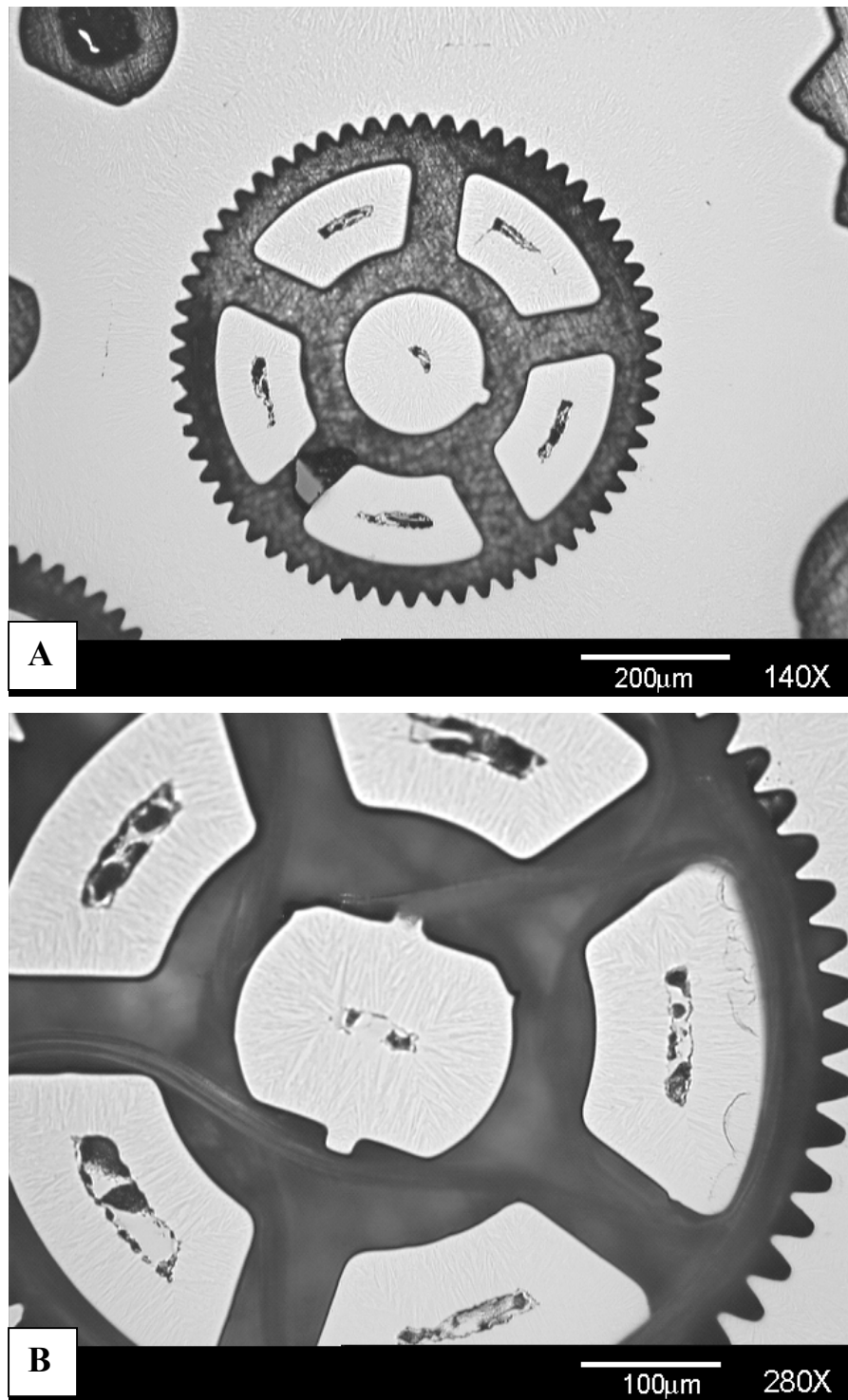
Figure 8a & b. Plan view, optical micrographs of different regions of polished electrodeposited Ni daughter piece. Some small voiding is present in all the features. The grain structure indicates film growth and evolution.

Metal Deposition on Conductive PMMA

The feature-filling performance of the deposition schemes listed in Table 1 was assessed by cross-sectioning the features after deposition. For the sample made with direct current, it was found that no metal was deposited within the features; it is not known if this was due to entrapped bubbles present before the deposition or by gas evolution during the deposition itself. Another possibility is the creation of a resin-rich layer during the hole drilling, resulting in a non-conductive surface in the feature. In any case, the same problem was encountered with the sample fabricated with pulse reverse deposition. Pulsed deposition resulted in metal distributed throughout the features as shown in the optical micrograph in Figure 9 somewhat non-uniformly; the features made by direct current with coumarin were similar in overall appearance and are not presented here. The feature-filling performance F was quantified by the following definition

$$F = \frac{d_{int}}{d_{ext}} \qquad (2)$$

where d_{int} is the deposited film thickness of the deposit halfway down the interior of the feature and d_{ext} is the deposited film thickness on the exterior of the feature as indicated in Figure 9.

Table 2 compares F values for each of the four electrodeposition schemes. Both pulsed deposition and direct current deposition resulted in interior thicknesses about 15% of that exterior of the feature. One interesting

aspect of the feature filling for pulsed deposition and deposition with a leveling agent is that the deposit thickness diminishes until ~300 μm into the feature, after which it remains approximately constant. This is consistent with the expectation that the Ni^{2+} concentration and the local deposition rate both diminish with the feature depth.
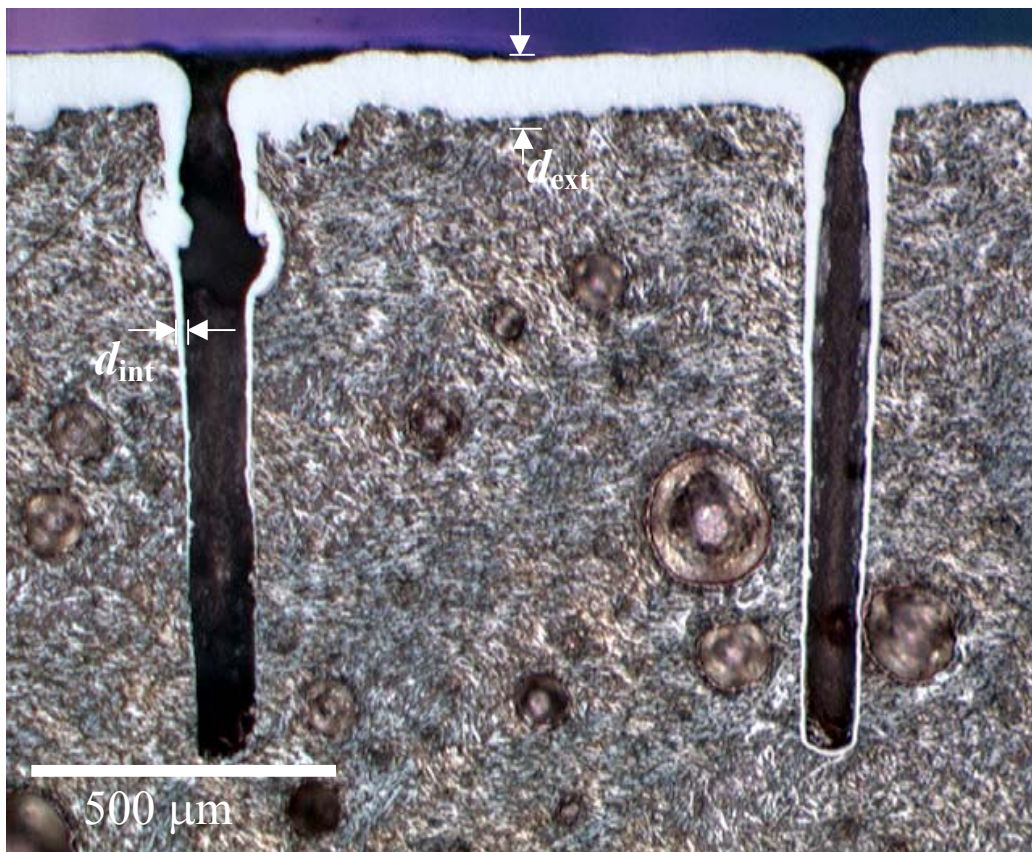
Figure 9. Cross-sectional optical micrographs of partially filled high-aspect ratio features drilled into conductive PMMA. Pulsed electrodeposition was used as described in Table 1 to deposit Ni. Since $t_{\text{off}} \ll \tau$, non-uniform filling results. Thicknesses to determine F are as indicated on the figure.

Scheme	F
Direct current	0
Pulsed deposition	0.15
Pulse reverse deposition	0
Leveling agent	0.16

Table 2. Feature filling performance of each electrolyte. Values were determined by taking the average for 5 features.

Due to the limitation on the maximum value for t_{off} in a chloride-free bath,[16] it was necessary that $t_{off} \ll \tau$. It was expected that the features would not be uniformly filled, but the extent to which the constraint on t_{off} would affect the non-uniformity was not known. Evidently from Figure 9, t_{off} must be significantly larger than the chosen value of 30 sec for this feature geometry, necessitating an alteration to the bath chemistry.[16] In principle, given an adequately long off-time and short on-time, features like those in Figure 9 may be filled in a void-free fashion. Assuming a $t_{on} \cong \tau/4$ and $t_{off} \cong \tau$, for example,[15] and keeping i_{on} constant at 15 mA/cm^2, it would take ~20 hours to fill a 150 μm wide feature. Future studies will consequently focus on chloride-containing electrolytes.

Although t_{off} scales with L^2 as discussed in the theory section, this does not mean that the total time to fill a feature does so as well. If the void-free

filling criterion is simply that $t_{on} \cong \tau/2$ and $t_{off} \cong \tau$,[15] it may be shown that recommended deposition rate is independent of PMMA thickness. The average current density (which is proportional to the deposition rate), determined by the charge per area Q passed over a pulse period, is

$$i = \frac{Q}{t} = \frac{i_{on} \cdot t_{on} + i_{off} \cdot t_{off}}{t_{on} + t_{off}} = i_{on} \frac{t_{on}}{(t_{on} + t_{off})} = i_{on}\phi \qquad (3)$$

where ϕ is the duty cycle. Thus, the average deposition rate does not depend on the individual lengths of the pulse but rather on i_{on} and the duty cycle. For example, τ for a 100 μm thick mold is ~10 sec, leading to t_{on} of 2.5 sec and t_{off} of 10 sec. With a i_{on} of 15 mA/cm², the deposition rate is ~ 3.7 μm per hour. For a 1000 μm thick mask, t_{on} = 250 sec and t_{off} = 1000 sec; ϕ and i_{on} are unchanged, resulting in a deposition rate of ~ 3.7 μm per hour. If ϕ can be kept constant by increasing the pulse on-times to accommodate long off-times for large PMMA thicknesses, the recommended deposition rate should be independent of mask thickness (although the total deposition time will not). We plan to test this predicted behavior in future studies.

Conclusions

Through-mask electrodeposition may be used to fill features with active sidewalls. The success of such an approach depends on the size of the features and the selection of deposition parameters, such as the current waveform and the presence of leveling agents. Pulsed deposition and employing leveling agents appeared to be better than pulse reverse plating at filling features with aspect ratios > ~7, while features having aspect ratios <2 were filled with only minor voiding with simple direct current. Required pulse off-times for thicker masks necessitate the use of electrolytes with chloride ions. Conductive plastic substrates appear to be more promising than metal substrates since demolding is problematic in the latter case.

References

1. M. Heckele, W. Bacher, and K. D. Mueller, *Microsystem Technologies*, **4**, 122 (1998).

2. M. S. Depsa, K. W. Kelly, and J. R. Collier, *Microsystem Technologies*, **6**, 60 (1999).

3. H. Becker and C. Gartner, *Electrophoresis*, **21** (1), 12 (2000).

4. A. Thies, V. Piotter, J. H. Hausselt, and O. F. Hagena, *Microsystem Technologies*, **4**, 110 (1998).

5. P. Gatz and O. F. Hagena, *Applied Surface Science,* **91**, 169 (1995).

6. R. Ruprecht, T. Benzler, T. Hanemann, K. Mueller, J. Konys, V. Piotter, G. Schanz, L. Schmidt, A. Thies, H. Woellmer, J. Hausselt, *Microsystem Technologies*, **4**, 28 (1997).

7. N. Rajan, M. Mehregany, C. A. Zorman, S. Stefanescu, and T. P. Kicher, *Journal of Microelectromechanical Systems*, **8** (3), 251 (1999).

8. L. Romankiw, *Electrochimica Acta*, **42**, 2985 (1997).

9. J. J. Kelly, C. Tian, and A. C. West, *J. Electrochem. Soc*., **146**, 2540 (1999).

10. J. J. Kelly and A. C. West, *Electrochemical and Solid State Letters*, **2**, 561 (1999).

11. C. Madore, M. Matlosz, and D. Landolt, *J. Electrochem. Soc*., **143**, 3927 (1996).

12. C. Madore and D. Landolt, *J. Electrochem. Soc.*, **143**, 3936 (1996).

13. J. W. Dini and H. R. Johnson, *Metal Finishing*, **68** (9), 52 (1970).

14. J. Newman, *Electrochemical Systems*, 2nd Ed., Prentice-Hall, New Jersey, 1991.

15. A. C. West, C. C. Cheng, and B. C. Baker, *J. Electrochem. Soc.*, **145**, 3070 (1998).

16. W. Kim and R. Weil, *Surface and Coatings Technology*, **31**, 143 (1987).

INITIAL DISTRIBUTION:

1	MS0139	R. Kreutzfeld, 2613		3	MS9018	Central Technical Files, 8945-1
1	MS0329	L. L. Lukens, 2614		1	MS0899	Technical Library, 9616
1	MS0329	M. A. Polosky, 2614		1	MS9021	Classification Office, 8511/Technical Library, MS0899, 9616 DOE/OSTI via URL
1	MS0139	C. W. Vanecek, 2613				
1	MS0889	B. L. Boyce, 1835				
1	MS0889	T. E. Buchheit, 1835				

1	MS9001	M. E. John, 8000; Attn:
	MS9002	P. N. Smith, 8500
	MS9003	K. E. Washington, 8900
	MS9004	J. Vitko, 8100
	MS9005	D. R. Henson, 2200
	MS9007	D. R. Henson, 8400
	MS9031	K. C. Olsen, 11600
	MS9054	W. J. McLean, 8300

1	MS9042	J. A. Crowell, 8727
1	MS9042	W-Y Lu, 8725
1	MS9401	J. M. Hruby, 8702
5	MS9401	J. T. Hachman, 8729
1	MS9401	D. E. McLean, 8729
1	MS9401	M. A. Bankert, 8729
1	MS9401	A. M. Morales, 8729
1	MS9401	R. Shediac, 8729
1	MS9401	C-Y P. Yang, 8729
1	MS9401	D. M. Skala, 8729
1	MS9401	R. P. Janek, 8729
1	MS9401	C. C. Henderson, 8729
5	MS9401	J. J. Kelly, 8729
1	MS9402	K. L. Wilson, 8724
1	MS9403	J. C. Wang, 8723
5	MS9403	N. Y. C. Yang, 8723
1	MS9404	S. H. Goods, 8725
1	MS9405	D. A. Hughes, 8726
1	MS9671	D. A. Chinn, 8729

1	MS9405	R. H. Stulen, 8700; Attn:
	MS9042	J. L. Handrock, 8727
	MS9042	M. F. Horstemeyer, 8728
	MS9161	E. P. Chen, 8726
	MS9161	R. Q. Hwang, 8721
	MS9401	J. R. Garcia, 8725
	MS9402	C. H. Cadden, 8724
	MS9403	W. R. Even, 8722
	MS9409	G. D. Kubiak, 8732
	MS9409	J. Goldsmith, 8730
	MS9409	W. C. Replogle, 8731